Journal of Mammary Gland Biology and Neoplasia (2019) 24:185–197
https://doi.org/10.1007/s10911-019-09427-1

Mammary Epithelial Cell Lineage Changes During Cow's Life

Laurence Finot[1] · Eric Chanat[1] · Frederic Dessauge[1]

Received: 27 November 2018 / Accepted: 27 January 2019 / Published online: 13 February 2019

Abstract

Milk production is highly dependent on the optimal development of the mammary epithelium. It is therefore essential to better understand mammary epithelial cell growth and maintenance from the related epithelial lineage during the animal life. Here, we characterized the epithelial lineage at puberty, lactation and dry-off in bovine using the cell surface markers $CD49_f$, CD24, and CD10. The pubertal period was characterized by a high proportion of $CD49_f^{pos}$ cells corresponding to various epithelial subpopulations, notably the $CD24^{pos}$ subpopulations. The proportion of $CD49_f^{pos}$ cells was weaker during lactation and dry-off, and $CD24^{pos}$ cells were relatively few. Of note, the (sub)population profile at dry-off appeared close to that during lactation. Using a targeted gene approach, we associated specific genes with epithelial subpopulations, their expression level varying, or not, according to physiological stages. *Caseins* were only expressed in the $CD49_f^{med}CD24^{neg}$ subpopulation. Basal marker genes (*keratin(KRT)5*, *KRT14* and *αSMA*) were found in the $CD49_f^{high}CD24^{neg}$ subpopulations. Luminal gene markers (*KRT7*, *KRT8* and *KRT19*, *CDH1* and the *PRLR*) were expressed in the $CD49_f^{low}CD24^{neg}$ subpopulation. The $CD49_f^{low}CD24^{pos}$ subpopulation, only abundant at puberty, expressed luminal gene markers and *KI67* at high level. In contrast to others, the $CD49_f^{high}CD24^{pos}$ cells accounted for a small proportion of total cells, decreasing from puberty to dry-off. They were characterized by expression of luminal and basal gene markers and low *KI67* level. Interestingly, this subpopulation showed a remarkable stability of gene expression profile throughout physiological stages and bear the hallmark of quiescence that designate them as the potential bovine mammary stem cells.

Keywords Mammary gland · Epithelial lineage · Stem cells · Bovine

Introduction

The mammary gland is a dynamic organ that experience different phases during the female life. Establishing the function of lactation and the management of the subsequent lactating cycles are accompanied by important morphological and functional changes. In cattle, morphogenesis of the mammary gland occurs during the embryogenesis but the main development takes place postnatally. A mammary epithelial rudiment develops as from birth and the epithelium grows and extends upon endocrine hormones and growth factors stimulation [1, 2]. The complex organization of the mammary epithelium is built throughout puberty by a process referred to as branching morphogenesis in which the ductal elongation and branching processes are driven by terminal ductal lobular units (TDLU) located at the ends of the growing ducts [3]. Two primary cellular lineages constitute the ducts and TDLUs: an inner cell layer (luminal cells) that surround the alveolar lumen and an outer cell layer of basal/myoepithelial cells that lie adjacent to the basement membrane. In bovine, the mammary tissue develops in a compact parenchymal mass constituted by the epithelial structures, ducts and alveoli, all surrounded by a dense matrix of connective tissue. During gestation, the epithelial lobulo-alveolar units form and mature in response to circulating hormones, notably prolactin (PRL) [4]. After parturition, the epithelium starts to be fully functional with terminal differentiation of the epithelial cells secreting milk proteins into the lumen of the lobular alveoli (acini). Following the cessation of lactation, the mammary gland involutes through mechanisms of apoptosis to regulate epithelial (mainly alveolar) cell number and mammary tissue remodeling via an extracellular matrix-degrading process and epithelial-mesenchymal or mesenchymal-epithelial transitions [5].

Electronic supplementary material The online version of this article (https://doi.org/10.1007/s10911-019-09427-1) contains supplementary material, which is available to authorized users.

✉ Frederic Dessauge
Frederic.dessauge@inra.fr

[1] PEGASE, INRA, Agrocampus Ouest , 35590 Saint-Gilles, France

After involution and epithelial tissue regression, the mammary gland reverts to a quiescent state waiting for the next pregnancy/lactation cycle that will see the re-appearance of a massive alveolar tissue. In addition to these processes, the mature mammary epithelial cells were estimated to undergo a turnover of 50% during a lactation period in bovine [6].

The existence of mammary stem cells (MaSC) and their progenitor in the mammary gland is needed to give birth to the various mature and differentiated cells that make up the tissue, both during its development and for tissue regeneration and homeostasis. Evidence came from in vivo transplantation assays in mice where cells isolated from the mammary gland were found to be capable of regenerating a whole gland when placed in a suitable mammary microenvironment [7]. Since then, MaSC were largely investigated in the mouse and human models. In contrast, bovine studies are scares. In a pioneer study, Ellis and Capuco (2002) identified a population of lightly stained cells with high proliferative capacity within the mammary parenchyma of heifer mammary gland. They suggested these cells to be the putative MaSC [8]. Next, Capuco (2007) delineated a putative bovine MaSC population on the basis of their ability to retain a DNA staining marker (Hoechst 33342). Because this cell population contained both estrogen receptors (ER)-positive and ER-negative cells, the authors suggested that the latter cells were stem cells while the former were progenitor cells [9]. More recently, Martignani et al. (2009) used the test of colony forming unit to study the clonogenic capacity of expansion of bovine MaSC and found three distinct colonies on the basis of their morphology and size. One colony exhibited a myoepithelial phenotype based on the expression of the cytokeratins (KRT) (KRT18- / KRT14+) while the other two had luminal characteristics (KRT18+ / KRT14-) [10]. Also using Hoechst 33342, Osinska et al. (2014) estimated the number of MaSC within a suspension of mammary epithelial cells (MEC) to account for 0.5% of the total cells of the bovine mammary gland [11]. In 2012, Rauner and Barash used a murine epithelial cell enrichment kit to obtain a pure population of epithelial cells. Subsequently, various subpopulations were defined on the basis of cluster of differentiation (CD) CD24 and $CD49_f$ expressions. Further analysis allowed them to propose a cell hierarchy and lineage commitment model. The putative stem cells defined by their basal origin, bipotent characteristic, and their capacity to form organized colonies at a high growth rate were put at the top of the hierarchy [12]. We recently highlighted putative MaSC in the lactating cows using the cell surface markers CD24 and $CD49_f$ [13]. Our more recent study using pubertal cows highlighted four populations present at high proportions in the mammary gland of heifers. Investigations of the functional properties and molecular characteristics of these populations allowed us to hypothesize that the $CD49_f^{high}CD24^{pos}$ cells is the MaSC population and the $CD49_f^{low}CD24^{pos}$ cells progenitors [14]. So far, studies concerning MaSC in cattle are mainly descriptive due to technological bottle necks. In contrast, the use of new technologies (e.g. lineage tracing experiments) in mouse models have helped to unravel the dynamics of MaSC during the postnatal morphogenesis of the mammary gland [3]. Indeed, it was possible to highlight that all cells within the postnatal mammary gland arise from unipotent long-lived (lineage-restricted) stem cells rather than multipotent stem cells [15, 16]. Consequently, the lineage-restricted stem cells would be responsible for the homeostasis of the mammary gland. Can we extrapolate these findings to other species, ruminants notably? Comparison of MaSC characteristics between species proved that interspecies differences exist and, unfortunately, the technological approaches implemented in mouse are hardly attainable in bovine [17].

Obviously, the mammary epithelium exhibits a considerable degree of cell fate plasticity during the lifetime. The orchestrated chain of events implicates the contribution of epithelial cell populations from the epithelial hierarchy. Mammary stem cells, luminal progenitors cells, basal progenitors cells, myoepithelial cells, luminal cells, alveolar cells, secretory epithelial cells, etc.… all participate in the morphological changes. These cells or cell populations can be discriminated from each other by different cell markers and/or their expression levels [18]. Up to date, flow cytometry has been extensively used to characterize the phenotype of epithelial cells such as MaSC/progenitors based on the expression of CD [19, 20]. Cells from the epithelial lineage were found to express CD29 or $CD49_f$ (α6 integrin) and the MaSC were defined by the co-expression of $CD49_f$ at high level and CD24 in numerous studies in mice, human and other mammals, including bovine [12, 17, 21–23]. To distinguish basal cells in the epithelial cell population we used CD10 which has been demonstrated to be a cell surface marker of basal cells in the bovine mammary tissue [14, 24], FACS sorting of the cell populations from the epithelial lineage led to define their features in term of phenotypic characteristics and gene expression profiles [12]. αSMA (Smooth muscle actin alpha), KRT5, KRT14, CD10, p63 and the intermediate filament vimentin are generally localized in the basal MEC (reviewed in [25]). Useful markers for identifying luminal cells include KRT7, KRT8, KRT19, CD24 and E-cadherin (CDH1). Several proteins as the leucine-rich repeat-containing G protein coupled receptor 5 (LGR5), Notch homolog 1 (NOTCH1) or protein C receptor (PROCR) were shown to be stem cell and/or progenitors markers. Expression of PROCR was found in cells of the basal compartment exhibiting same regenerative capacities than MaSC in the postnatal mammary gland for PROCR lineage tracing experiment [26, 27].

Extensive studies have been carried out in the murine model mainly on the mammogenesis from the prenatal to the postnatal development. But little is known about the evolution of the epithelial lineage from development to dry-off in other mammals. To date, our understanding of the bovine MaSC/progenitors evolution in number and phenotypic characteristics is limited. In this context, we first defined the distinct mammary epithelial cells subpopulations committed to the mammary epithelial development at puberty by multiple criteria as classical cell surface marker expression ($CD49_f$ and CD24) using flow cytometry [14]. These epithelial cells subpopulations were characterized by their in situ localization, phenotypic characteristics and gene expression signature. Here, we have deepened our knowledge of mammary tissue development in bovine by comparing the epithelial lineage, focusing on the MaSC/progenitors, on the basis of the phenotypic characteristics and molecular signatures of the epithelial subpopulations between puberty, lactation and dry-off, i.e. between the key physiological periods in cow's life.

Results

Epithelium Organization at Key Stages of Cow's Life

Our experimental approach was to explore first the morphology of the mammary tissue to apprehend the organization of the epithelium and the epithelial cell types at three physiological key stages: 17-months old cow (PC), multiparous lactating cows (LC) and dried cows (DC). Hematoxilin and eosin staining revealed the gross morphology of the mammary tissue, allowing visualization of the stroma, referred to as the connective tissue including vascular tissue (pink colored tissue). Adipose tissue was visualized separately from the stromal tissue (white tissue) and the epithelium (comprising ducts and alveoli) appeared as the purple colored tissue (Fig. 1a). The lobulo-alveolar and acini structures were observed and quantified separately (epithelial area), taking into account the area of the acini lumen. At puberty (Fig. 1a; PC), the mammary neo-structures in expansion drive invasive ductal

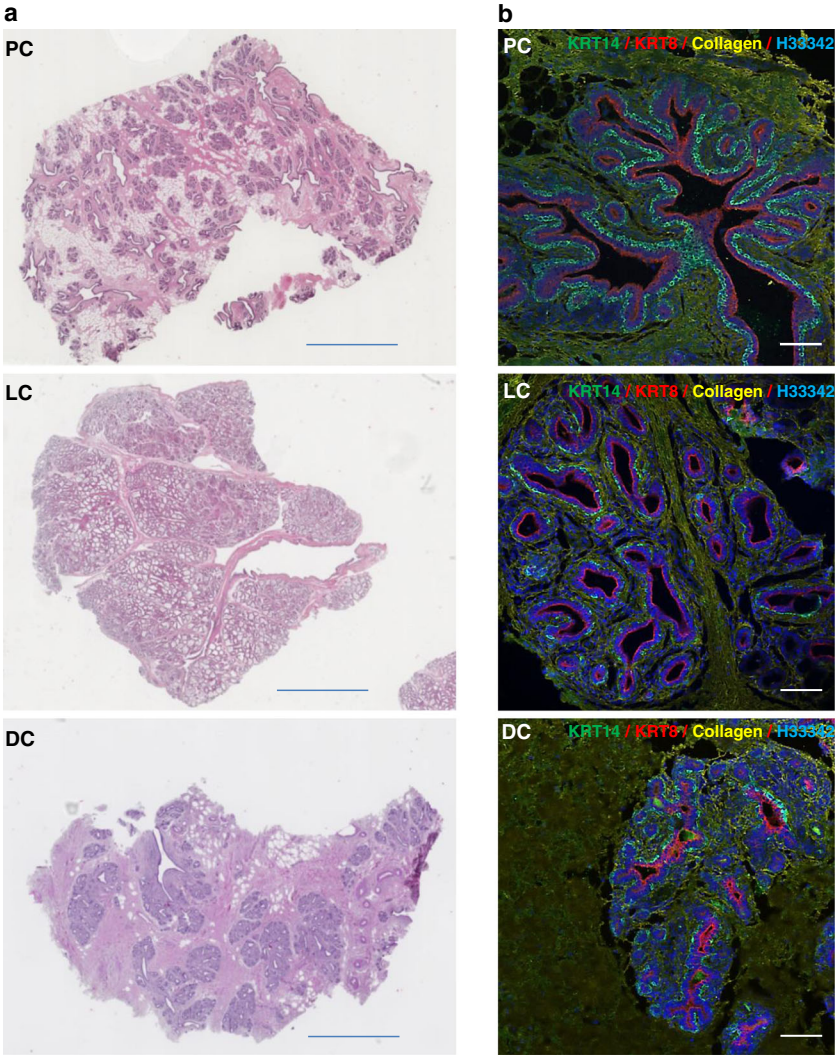

Fig. 1 Morphology and cellular organization of the bovine mammary tissue of pubertal PC), lactating (LC) and dried cows (DC). **a** Hematoxylin and Eosin staining of mammary tissue sections visualized using a nanozoomer microscope. Images are representative of the animals at the indicated physiological stage. Scale bar = 2 mm. **b** Quantification of tissular and cellular structures in the bovine mammary tissue. Results are generated from the nanozoomer representative images (one image per each cow) displayed in (**a**). Stromal, adipose, epithelial tissues and acini areas were determined using Image J macros. Data are expressed as the mean percentage ± SEM ($n = 3$ for PC; $n = 4$ for LC and n = 3 for DC) of specific tissue area relative to the total surface of the tissue section. Different letters (**a**-**b**) indicate significant differences ($p < 0.05$). **(c)** Immunofluorescence staining of the basal marker keratin 14 (KRT14, green); the luminal marker keratin 8 (KRT8, red) and the stromal marker collagen type I (Collagen, yellow) within the mammary tissue slices. Nuclei are stained with Hoechst 33342 (blue). Scale bar = 100 μm

branching throughout the mammary stroma and fat pad. The epithelium accounted for 28% of the total section area (Table 1) whilst the majority of the tissue was stromal (57%). The structuration into lobules and acini was not well defined yet. Immunofluorescence staining for basal and luminal cells by KRT14 and KRT8, respectively, highlighted the relative localization of the epithelial cell types engaged in the mammary structures during development (Fig. 1b). Round cells expressing the KRT14 clearly surrounded the developing duct structures, cells labeled by KRT8 forming the inner layers. Buds of luminal cells appeared on lateral sides of the duct and in some TDU. These luminal and basal cells were committed to the elongation and branching of the ductal structure during this pubertal period. During lactation, the morphology of the mammary tissue was well structured in lobes and lobules (Fig. 1a, LC) with a clear distinction of the acini and alveoli lumen. The epithelium accounted for the majority of the tissue (58% of the total area) while acini occupying 65% of the total area whereas the stroma and the adipose tissues make 38% and 3.6% of the total section area, respectively (Table 1). Acini were constituted by a monolayer of luminal cells expressing KRT8 surrounded by a monolayer of outer elongated cells, the latter being weakly stained at their basal side by the anti-KRT14 antibodies (Fig. 1b, LC). In the mammary tissue of dried cows, lobes were small and distinct, separated by large areas of dense stromal tissue containing collagen; few alveolar lumens were visible (Fig. 1a, DC). The stromal tissue stood for 75% of the total section area (Table 1). The epithelium, however, still accounted for 22% of the total section area. Immunofluorescence showed that the mammary structures observed within the lobes were mainly ducts with open lumen lined by cells expressing KRT8 and round cells expressing KRT14 within the outer layer of the ductal structures (Fig. 1b, DC). Acini appeared small and nearly regressive.

Table 1 Tissues and acini proportions (in %) determined from histologic mammary sections stained by hematoxylin and eosin in pubertal (n = 3), lactating (n = 4) and dried cows (n = 3)

	Pubertal cows	Lactating cows	Dried cows
Stromal tissue	57.8 ± 4.7^{a}	38.7 ± 4.8^{b}	75.7 ± 4.1^{a}
Adipose tissue	16.8 ± 8.1^{a}	3.6 ± 0.6^{a}	2.1 ± 0.6^{a}
Epithelial tissue	28.4 ± 3.7^{b}	58.1 ± 4.4^{a}	22.1 ± 4.3^{b}
Acini	27.5 ± 3.3^{a}	65.1 ± 3.9^{b}	25.1 ± 4.9^{b}

Data correspond to the mean percentage ± SEM of each type of tissue area related to the total mammary area. Stromal, adipose and epithelial tissues measured from the histological staining detailed in the corresponding Fig. 1, accounted for 100%. Acini were determined separately. Different letters (a-c) indicate statistically significant ($p < 0.05$) differences between each mean value

Comparison of the Epithelial Subpopulations at Three Key Physiological Stages

In order to further characterize the MEC at key physiological stages, we investigated the expression of $CD49_f$, CD24 and CD10 within total single cell suspension dissociated from the mammary tissue of PC, LC and DC cows using flow cytometry. First, we evaluated the epithelial populations expressing either $CD49_f$, CD24 or CD10 (Fig. S1 and Table 2), then the subpopulations co-expressing these cell surface proteins (Fig. S2 and Table 3). As detailed in Table 2, the majority of the cells dissociated from the mammary tissue in development were $CD49_f^{pos}$ (62.3% ± 4%). Those were in much lower amount in tissue taken during lactation or dry-off (23.3% ± 2.1% or 36.5% ± 8.9%, respectively), the later differences being not significant. Similar differences were made regarding cells expressing CD24, this subpopulation being relatively abundant in the mammary tissue in development (23.2% ± 4.6%) but poorly present during lactation (4.9% ± 0.7%) and dry-off (1.7% ± 0.5%), with no significant differences between these two stages. As to the CD10 subpopulation, it represented almost half of the total mammary single cells (43.8% ± 7.7%) in the mammary tissue in development. This proportion was drastically reduced at lactation with only 5.5% ± 0.7% of the cells expressing this marker whereas it accounted for 27.5% ± 3.4% at dry-off.

We next analyzed the occurrence of co-staining for the two cell surface markers $CD49_f$ and CD24 in order to further delineate the different subpopulations constituting the epithelial lineage. As shown in Fig. 2, top left panel, the cytometric profiles for $CD49_f$ and CD24 expression in PC displayed four distinct subpopulations. Within the $CD49_f^{pos}$ cells (65%), most were $CD49_f^{pos}CD24^{neg}$ (43.3% ± 2.8%) and equally distributed into two distinct subpopulations, the $CD49_f^{low}CD24^{neg}$ (19.8% ± 1.2%) and $CD49_f^{high}CD24^{neg}$ (22.1% ± 1.6%), as detailed in Table 3. A third subpopulation, the $CD49_f^{low}CD24^{pos}$ cells, was relatively highly represented

Table 2 Flow cytometry analyses for $CD49_f$, CD24 and CD10 expression on single cells dissociated from mammary tissue of pubertal cows (PC), lactating cows (LC) and dried cows (DC)

Populations	PC*	LC	DC
$CD49_f^{pos}$	62.3 ± 4.0^{a}	23.3 ± 2.1^{b}	36.5 ± 8.9^{b}
$CD24^{pos}$	23.2 ± 4.6^{a}	4.9 ± 0.7^{b}	1.7 ± 0.5^{b}
$CD10^{pos}$	43.8 ± 1.7^{a}	5.5 ± 0.7^{c}	27.5 ± 3.4^{b}

Mammary single cells obtained after tissue digestion and cell dissociation were stained with anti-$CD49_f$, -CD24 and -CD10 antibodies (triple staining). Data correspond to the mean percentage ± SEM of cells for each single staining. Different letters (a-c) indicate statistically significant ($p < 0.05$) differences between each mean value. Asterisk: data were previously published [14]

Table 3 Flow cytometry analyses for CD49f, CD24 and CD10 co-expression in mammary tissue of pubertal (PC), lactating (LC) and dried (DC) cows

	PC*	LC	DC
$CD49_f$ /CD24 (sub-)populations			
$CD49_f^{neg}$ $CD24^{neg}$	32.5 ± 5.2^{b}	64.6 ± 3.6^{a}	48.4 ± 8.8^{ab}
$CD49_f^{neg}$ $CD24^{pos}$	2.2 ± 0.1^{a}	1.6 ± 0.4^{ab}	0.6 ± 0.2^{b}
$CD49_f^{pos}$ $CD24^{neg}$	43.3 ± 2.8^{a}	30.8 ± 4.0^{b}	47.6 ± 8.8^{ab}
$CD49_f^{low}$ $CD24^{neg}$	19.8 ± 1.2	21.2 ± 2.4	28.7 ± 7.0
$CD49_f^{med}$ $CD24^{neg}$	1.4 ± 0.2^{b}	7.2 ± 1.6^{a}	7.1 ± 1.6^{a}
$CD49_f^{high}$ $CD24^{neg}$	22.1 ± 1.6^{a}	2.4 ± 0.9^{c}	11.7 ± 1.8^{b}
$CD49_f^{pos}$ $CD24^{pos}$	21.9 ± 3.7^{a}	3.0 ± 0.6^{b}	3.4 ± 0.2^{b}
$CD49_f^{low}$ $CD24^{pos}$	18.6 ± 3.4^{a}	1.6 ± 0.4^{c}	3.0 ± 0.3^{b}
$CD49_f^{high}$ $CD24^{pos}$	3.3 ± 0.3^{a}	1.5 ± 0.5^{b}	0.4 ± 0.0^{b}
$CD49_f$ /CD10 populations			
$CD49_f^{neg}$ $CD10^{neg}$	30.8 ± 2.7^{c}	74.5 ± 2.8^{a}	52.3 ± 7.0^{b}
$CD49_f^{neg}$ $CD10^{pos}$	10.3 ± 1.9^{a}	2.3 ± 0.5^{b}	9.5 ± 2.4^{ab}
$CD49_f^{pos}$ $CD10^{neg}$	25.4 ± 1.6	21.0 ± 2.4	9.6 ± 3.8
$CD49_f^{pos}$ $CD10^{pos}$	33.5 ± 1.6^{a}	2.1 ± 0.3^{c}	18.5 ± 3.1^{b}
CD10 /CD24 populations			
$CD10^{neg}$ $CD24^{neg}$	49.5 ± 2.4^{c}	90.5 ± 0.4^{a}	70.8 ± 3.3^{a}
$CD10^{neg}$ $CD24^{pos}$	6.7 ± 1.7^{a}	4.0 ± 0.5^{ab}	1.7 ± 0.5^{b}
$CD10^{pos}$ $CD24^{neg}$	29.0 ± 4.1^{a}	3.2 ± 0.5^{b}	25.4 ± 3.2^{a}
$CD10^{pos}$ $CD24^{pos}$	14.8 ± 3.2^{a}	2.3 ± 0.3^{b}	2.1 ± 0.3^{b}
CD10 expression in the CD49f and CD24 (sub-)populations			
$CD49_f^{neg}$ $CD24^{neg}$	26.4 ± 4.0^{a}	1.5 ± 0.4^{b}	17.2 ± 0.9^{a}
$CD49_f^{low}$ $CD24^{neg}$	8.3 ± 1.0^{b}	6.4 ± 1.8^{b}	25.1 ± 12.6^{a}
$CD49_f^{med}$ $CD24^{neg}$	*Not present*	8.8 ± 3.9	33.9 ± 11
$CD49_f^{low}$ $CD24^{pos}$	90.4 ± 4.0^{a}	69.1 ± 3.9^{b}	76.1 ± 11.8^{ab}
$CD49_f^{high}$ $CD24^{neg}$	90.2 ± 2.4^{a}	40.1 ± 1.8^{b}	85.5 ± 4.1^{a}
$CD49_f^{high}$ $CD24^{pos}$	93.1 ± 0.9^{a}	77.1 ± 4.8^{b}	85.7 ± 7.7^{ab}

Mammary single cells obtained after tissue digestion and cell dissociation were stained with anti-CD49f, -CD24 and -CD10 antibodies (triple staining). Data correspond to the mean percentage ± SEM of cells for each multiple staining (in the case of CD10 expression results). Different letters (a-c) indicate statistically significant ($p < 0.05$) differences between each mean value. The asterisk indicates that data of pubertal cows was previously published in 2018 [14]

with 18.6% (± 3.4%) of the total cells whereas the fourth subpopulation, the $CD49_f^{high}CD24^{pos}$ cells, accounted for 3.3% (± 0.3%) of the total cells. In the LC, the $CD49_f^{pos}$cells were essentially $CD49_f^{pos}$ $CD24^{neg}$ as display in the cytometric profile of Fig. 2. Very few cells co-expressed $CD49_f$ and CD24 (3% ± 0.6%). From the 30.8% (± 4%) of the $CD49_f^{pos}CD24^{neg}$ population, the $CD49_f^{low}CD24^{neg}$ cells accounted for 21.2% (± 2.4) whereas a medium subpopulation of $CD49_f^{med}CD24^{neg}$ represented 7.2% (± 1.6%). The smaller subpopulation was the $CD49_f^{high}CD24^{neg}$ cells with 2.4% (± 0.9%). Interestingly, the proportion of both the $CD49_f^{pos}CD24^{neg}$ and $CD49_f^{pos}CD24^{pos}$ cells significantly decreased during lactation as compared to the pubertal development stage. Finally, in DC it was possible to discriminate two distinct subpopulations from the $CD49_f^{pos}CD24^{neg}$ subpopulation, the $CD49_f^{low}CD24^{neg}$ (28.7% ± 7%) and the $CD49_f^{high}CD24^{neg}$ cells (11.7% ± 1.8%). Although the proportion of $CD49_f^{pos}CD24^{pos}$ cells (3.4% ± 0.2%) clearly differed from the pubertal period, it did not vary as compared to the lactating period.

To better visualize the diversity encountered in the epithelial lineages between the various physiological stages, graphs displaying the proportion of each (sub)populations based on $CD49_f$ and CD24 co-expression were drawn (Fig. 2, right panels). This highlighted that the pubertal period is characterized by a high proportion of $CD49_f^{pos}$ cells and a strong presence of epithelial subpopulations, especially the $CD24^{pos}$ subpopulations. The lactation period was characterized by a weaker proportion of $CD49_f^{pos}$ populations and a majority of $CD49^{low}$ and $CD49^{med}$ cells. In contrast, the $CD24^{pos}$ subpopulations were not well represented during the dried period. Of note, the profile of the (sub)populations at dry-off appeared close to that observed during lactation with few $CD24_f^{pos}$ subpopulations and similar $CD49_f^{pos}$ subpopulations.

Molecular Signature of the Epithelial Subpopulations at Puberty, Lactation and Dry-Off

Having identified the various mammary epithelial subpopulations at the key physiological stages of the cow's life, we next try to deeper characterize their phenotype and to compare them between stages. With this aim, we first determine the molecular signature of these subpopulations using a targeted gene expression approach, subjecting sorted cells cDNA to the Wafergen RT-qPCR technology (Fig. 3). It should be noted, however, that we were unable to sort subpopulations with too few cells or disparate cells close to abundant subpopulations. These missing subpopulations were the $CD49_f^{low}CD24^{pos}$ subpopulations of lactating and dried cows, the $CD49_f^{high}CD24^{neg}$ of lactating cows and the $CD49_f^{med}CD24^{neg}$ of pubertal and dried cows. Target genes were mostly chosen on the basis of their putative role in the differentiation of the epithelial phenotype and lactation function. They included genes encoding cytoskeleton components such as keratins and vimentin or adhesion proteins (occludin and epithelial cadherin), putative stem cell markers (NOTCH1, ALDH1 or LGR5), receptivity to hormones (estradiol, progesterone or prolactin receptors) or growth factors (insulin growth factor receptor), and mammary cell activity (caseins, collagen or matrix metalloprotease 2). A set of genes was chosen for their involvement in epigenetic function as the DNA methyl transferases (DNMT). Principal component analysis (PCA) of the RT-qPCR data demonstrated that set of genes are correlated to distinct epithelial subpopulation. Indeed, the $CD49_f^{med}CD24^{neg}$ subpopulation was clearly related to the expression of the *β- and κ-caseins,* as

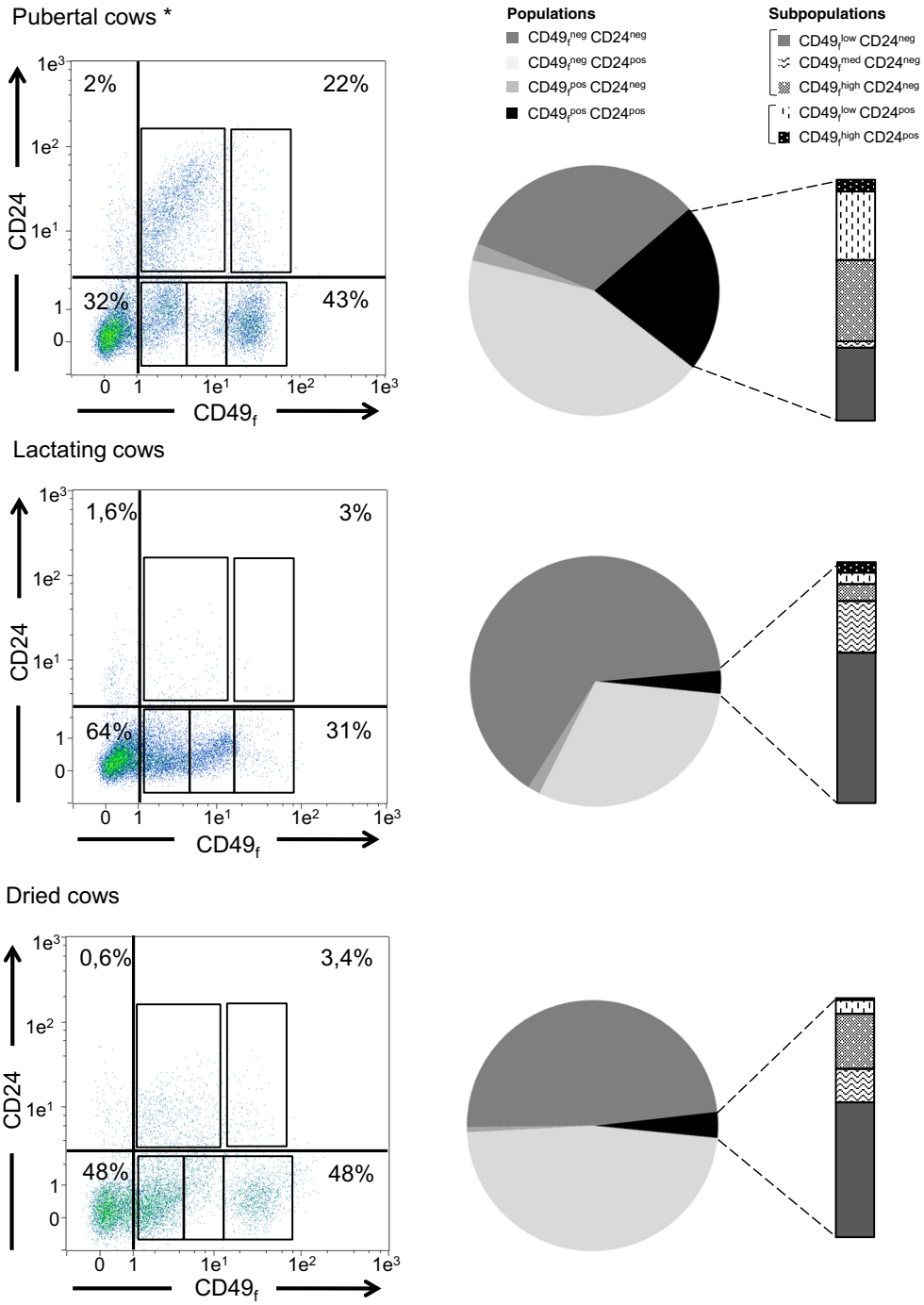

Fig. 2 Epithelial cell subpopulations at puberty, lactation and dry-off in the bovine mammary gland. Dissociated cells from the mammary tissue of pubertal, lactating and dried cows were co-stained with either $CD49_f$–FITC ($CD49_f$) and anti-CD24-APC (CD24), and analyzed by flow cytometry. In the flow cytometry dot-plots (left panels), each gating shows the positive cells located to the right of the gating on the x-axis and above the gating on the y-axis. The mean percentage of cells within each quadrant is indicated. Windows within positive areas of the plot define cell subpopulations. Asterisk: data plot previously published [14]. The relative proportions of epithelial populations (sector graph) and subpopulations constituting the $CD49_f^{pos}CD24^{pos}$ population (cumulative bar graph) are shown (right panels). Data are the mean percentage of n = 3 (pubertal cow), n = 4 (lactating cow) or *n* = 3 (dried cow) animals. The mean percentages of cells (± SEM) expressing CD10 or showing ALDH1 activity in each sub-population from three independent experiments (3 cows) are summarized in a table

well as *α-lactalbumin,* genes (Fig. 3a). On the other hand, several genes were correlated to the $CD49_f^{high}CD24^{neg}$ subpopulations. Those included *KRT5* and *KRT14*, *Maspin*, *αSMA*, *fibrobrast growth factor receptor or FGFR*, *β-catenin* and, of course, *CD49f*. Some of these genes did not vary whatever the physiological stage like $CD49_f$, *Maspin* and *KRT14* (Supplemental Table S1). In contrast, significant differences in gene expression were found according to the physiological stage. For example, *KRT5* was more expressed at puberty than at dry-off (Fig. 3b). Contrariwise, αSMA, β-catenin and FGFR mRNA were more abundant at dry-off. We found that the $CD49_f^{low}CD24^{neg}$ subpopulation was defined by expression of a set of KRT genes, namely *KRT7*, *KRT8, KRT18* and *KRT19*, together with *occludin*, *CDH1* and the *PRL receptor (PRLR)* genes (Fig. 3a). *KRT7* was expressed at similar levels whatever the physiological stage while others genes varied (Supplemental Table S1). Indeed, *KRT18* and *PRLR* were more abundant at puberty and decreased at lactation and dry-off whereas *KRT19* decreased significantly only at dry-off (Fig. 3c). In contrast, *the*

transforming growth factor receptor 1 (TGFbR1), oxytocin receptor (OXTR), insulin-like growth factor 1 receptor (IGF1R) and *GATA3* were more expressed in dried cows. One of the epithelial subpopulation which was strongly present at puberty and rare at the other physiological stages is the $CD49_f^{low}CD24^{pos}$ cell population. It was defined by a moderate abundance of *CDH1*, *KRT7*, *occludin* and *PRLR* genes (see supplemental Table 1). In this subpopulation, the proliferation protein marker *KI67* was overexpressed (Fig. 3d). In the PCA graph, the $CD49_f^{high}CD24^{pos}$ subpopulations were distributed close to the $CD49_f^{low}$ subpopulations. Those cell subpopulations shared the expression of *KRT8* and *CDH1* (Fig. 3a). In Fig. 3e, we focused on the $CD49_f^{high}CD24^{pos}$ cell subpopulation and make a visual graph based on the qPCR expression values to compare the expression profiles for the 48 genes, at the three physiological stages. This highlighted the similarity of the expression profiles through the three physiological stages. As shown in Fig. 3d, this subpopulation under-expressed *KI67*, at least during lactation and dry-off. An additional population appeared on the PCA graph which was defined by the expression of *the matrix metallopeptidase 2 (MMP2), Col1A1, TGFbR2, DNA methyltransferase 3b (DNMT3b)* and *vimentin* genes, with a slight decrease during lactation, as well as by the absence of expression of the targeted keratins (Fig. 3a and Supplemental Table S1). We concluded that this gene profile was most likely linked to the stromal cell population.

Finally, we determined the expression of CD10, a marker of the basal lineage, in these subpopulations by a triple staining in flow cytometry with $CD49_f$ and CD24 (Table 2). We observed that the $CD49_f^{low}CD24^{pos}$, and both the $CD49_f^{high}CD24^{neg}$ and $CD49_f^{high}CD24^{pos}$ subpopulations, expressed CD10 but with some differences according to the physiological stages. At puberty or at dry-off, CD10 expression was a phenotypic characteristic of the three subpopulations (nearly 90% to 93% and 76.1% to 85.7% respectively for the pubertal and dry-off periods). In contrast, during lactation CD10 expression decreased significantly for all three subpopulations.

Discussion

Depending on the physiological stages, the epithelial lineage varies and cells acquire phenotypic characteristics in line with the functional activity of the mammary gland. In the present study, we used flow cytometry and cell sorting based on the expression of the classical cell surface markers $CD49_f$, CD24 and CD10 to analyze and discriminate populations of the epithelial cell lineage. In addition, we compared the relative proportion of each epithelial subpopulation at three key physiological stages (puberty, lactation and dry-off), as well as their phenotypic and molecular characteristics at each age. This strategy allowed us to discern the potential effects of the physiological age-related status on epithelial cell fates. Nowadays, few is known about the epithelial lineage fate with age in bovine and the present literature essentially concerns the human and murine models. However, knowing the fate of the MaSC responsible for alveolar regeneration during the reproductive and lactation cycles is of utmost interest to apprehend the intrinsic capacity of the mammary tissue to regenerate epithelium with age. Yet, this is a major agronomic issue in milk-producing animals.

We defined the mature cells through the expression of the specific keratins and the well-known cell type markers CD10, or *Maspin*, using both of the latter markers for the basal lineage. From our results, one can conclude that the $CD49_f^{high}CD24^{neg}$ cell subpopulation matched the basal/myoepithelial cells. Of note, the number of this cell sub population varied at each physiological stage: they were relatively abundant at puberty (22%), drastically decreased during lactation (2%) and of intermediary proportion (11%) at dry-off. We believe that the relatively strong presence of basal cells at puberty was due to the fact that this cell type is dedicated to ductal elongation, a process that mostly occurs during this stage [28]. During lactation, basal cells were few. This might be due to the phenotypic changes that would occur during progressive differentiation and transformation of the basal cells into myoepithelial cells, those acquiring contractile proteins like αSMA and contractile function as previously depicted for the basal/myoepithelial cells in rat [29]. This is supported by the weak expression of CD10 we found in the $CD49_f^{high}CD24^{neg}$ cells during lactation. Indeed, it was previously described in bovine that myoepithelial cell differentiation is accompanied by both a decrease of CD10 and an increase of smooth actins expression [24]. Interestingly, the pool of basal cells was proportionally more abundant at dry-off than during lactation. These data are in agreement with the notion that at drying the epithelial tissue involutes with especially a regression of the lobulo-alveolar tissue mostly due to the reduction of the lumen size and secretory luminal cells, but with the conservation of the general structure (alveolus and ducts) of the tissue. In dairy cow, changes of the mammary tissue during involution are not as extensive as in other species, e.g. rodents, and the mammary tissue does not return to a "virgin" state. This might be due to the fact that cows are usually pregnant already during involution and pregnancy might play a role in the inhibition of the massive apoptosis of epithelial cells that would normally occurs during involution [30]. Our morphological observations and quantitative results were in accordance with such an evolution of the tissue organization. On the other hand, we were unable to compare the molecular signature of the $CD49_f^{high}CD24^{neg}$ cells during lactation to that of pubertal and dried cows due to the poor proportion of this subpopulation at that period. We found, however, that the basal/myoepithelial cells exhibited a

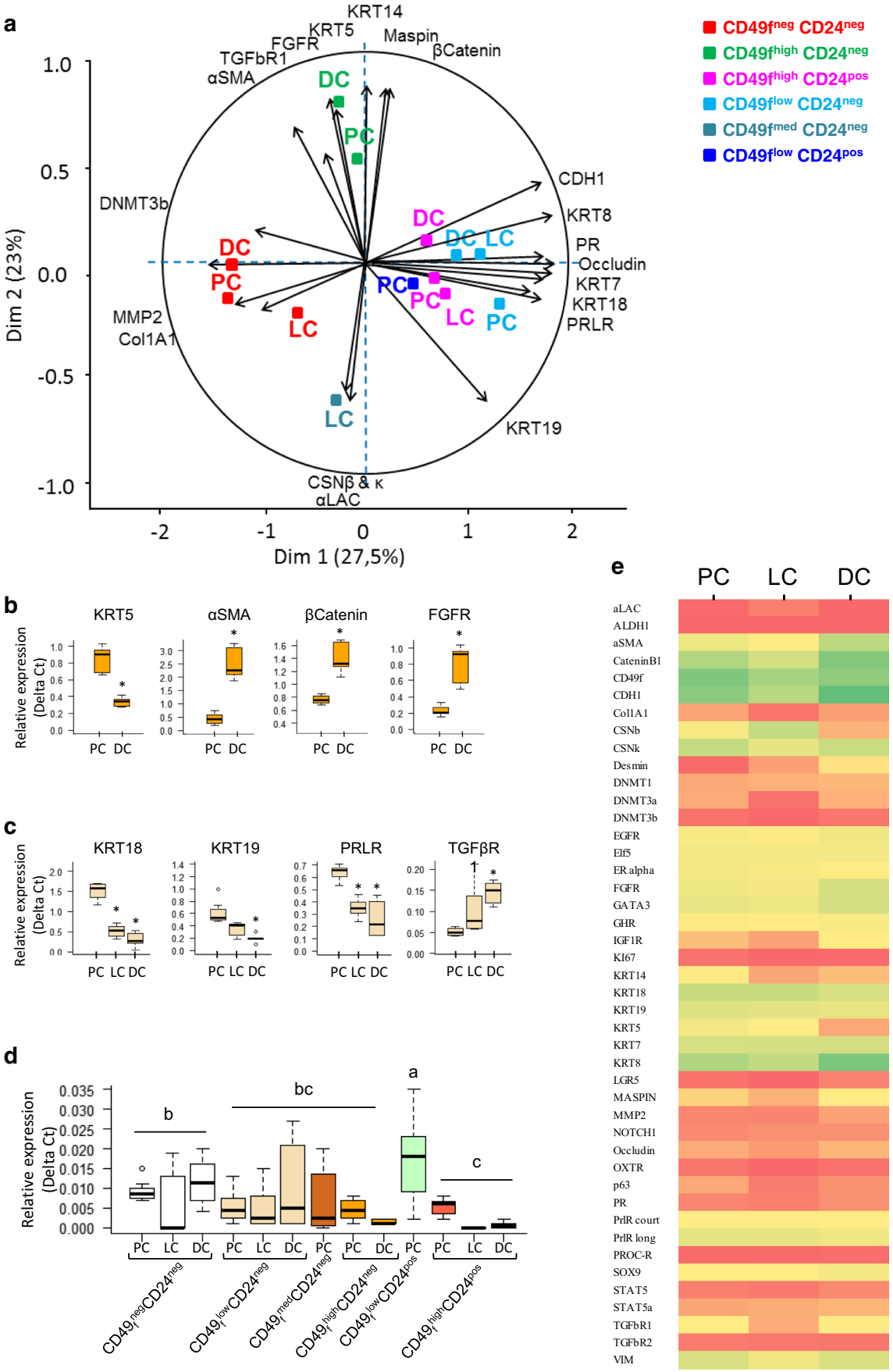
a
KRT14
KRT5
Maspin
FGFR
βCatenin
TGFbR1
αSMA
DC
PC
CDH1
DNMT3b
KRT8
DC
DC LC
PR
Occludin
DC
PC
PC
PC
LC
PC
KRT7
KRT18
PRLR
MMP2
Col1A1
LC
LC
KRT19
CSNβ & κ
αLAC
Dim 2 (23%)
Dim 1 (27,5%)
CD49f^neg CD24^neg
CD49f^high CD24^neg
CD49f^high CD24^pos
CD49f^low CD24^neg
CD49f^med CD24^neg
CD49f^low CD24^pos
b
KRT5
αSMA
βCatenin
FGFR
Relative expression (Delta Ct)
PC DC
c
KRT18
KRT19
PRLR
TGFβR
PC LC DC
d
Relative expression (Delta Ct)
b
bc
a
c
CD49f^negCD24^neg
CD49f^lowCD24^neg
CD49f^medCD24^neg
CD49f^highCD24^neg
CD49f^lowCD24^pos
CD49f^highCD24^pos
e
PC LC DC
aLAC
ALDH1
aSMA
CateninB1
CD49f
CDH1
Col1A1
CSNb
CSNk
Desmin
DNMT1
DNMT3a
DNMT3b
EGFR
Elf5
ER alpha
FGFR
GATA3
GHR
IGF1R
KI67
KRT14
KRT18
KRT19
KRT5
KRT7
KRT8
LGR5
MASPIN
MMP2
NOTCH1
Occludin
OXTR
p63
PR
PrlR court
PrlR long
PROC-R
SOX9
STAT5
STAT5a
TGFbR1
TGFbR2
VIM

◀ **Fig. 3** Gene expression profiles of epithelial subpopulations during puberty, lactation and dry-off. Cells dissociated from the bovine mammary tissue of pubertal cows (PC) ($n = 3$), lactating cows (LC) ($n = 4$) and dried cows (DC) (n = 3) were co-stained with anti-$CD49_f$ - FITC ($CD49_f$) and anti-CD24-APC (CD24) antibodies. The, cell subpopulations were sorted and the expression level of the targeted genes was measured in each subpopulation by RT-qPCR. **a** Graphical analysis of the gene expression profiles by Principal component analysis (PCA) statistical test. Each arrow represents the indicated gene. Correlation of genes and associated subpopulations is established by both the length and direction of the arrows. The proximity (same direction and length) of gene arrows with a subpopulation arrow indicates is representative of their level of correlation. **b** Boxplots depicting the expression level of the indicated genes by the $CD49_f^{high}CD24^{neg}$ subpopulation. *$P < 0.05$. **c** Boxplots depicting the expression level of the indicated genes by the $CD49_f^{low}$ $CD24^{neg}$ subpopulation. *$P < 0.05$. **d** Boxplot of the level of expression of the KI67 gene in the epithelial subpopulations. Different letters (a-c) indicate significant differences ($p < 0.05$). **e** Heat map graph of the level of expression of 48 genes in the $CD49_f^{high}CD24^{pos}$ subpopulation at puberty, lactation and dry-off. The color intensity is proportional to the level of gene expression based on the Delta Ct data. CSN, casein; CDH1, E-cadherin; Col1A1, collagen type 1; DNMT, DNA (cytosine-5)-methyltransferase; EGFR, Epidermal growth factor receptor; FGFR, Fibroblast growth factor receptor; KRT, keratin; αLAC, α-Lactalbumin; MMP2, Matrix metalloproteinase 2; PR, Progesterone receptor; PRLR, prolactin receptor; αSMA, Smooth muscle actin; TGFβR, Transforming growth factor receptor

different molecular signature at puberty as compared to dry-off, this later period being characterized by an overexpression of *αSMA, GATA3, βcatenin and FGFR*.

We recovered the luminal cells in the $CD49_f^{low}$ cell subpopulations. These clearly expressed the luminal keratins *KRT7, 8, 18* and *19*, as well as *CDH1*. Interestingly, the $CD49_f^{med}CD24^{neg}$ cell subpopulation clearly appeared during lactation and was the unique subpopulation that overexpress the caseins (*CSNb* and *k*) and the *α-lactalbumin* genes. We therefore concluded that this subpopulation contained the secretory epithelial cells. Of note, their relative proportion did not vary significantly between lactation and dry-off.

The most abundant luminal subpopulation contained the $CD49_f^{low}CD24^{neg}$ cells. Their proportion did not vary between physiological stages but their molecular characteristics did. Of note, the basal cell surface marker protein CD10 was not express at both puberty and lactation but was present at dry-off. This could suggest a conversion of these cells from the luminal to the basal/myoepithelial lineage after lactation, as was described in human during aging, with luminal cells acquiring molecular characteristics normally observed in myoepithelial cells (KRT14, integrin α6) and loosing the expression of the luminal marker KRT19 [31]. Here we showed that the luminal cells under-expressed *KRT8* and *KRT19* during dry-off but overexpressed *OXTR*, normally present in the myoepithelial cells, thus evoking a luminal-to-basal phenotypic change. In line with this, we showed that the changes in hormones and/or growth factors receptivity of the luminal cell subpopulation $CD49_f^{low}$ $CD24^{neg}$ is what distinguished them the most between physiological stages. During puberty, these cells were shown to express the *ERα*, *PR, PRLR* and *the growth hormone receptor*. These types of hormones are known to intervene in the process of branching morphogenesis during the pubertal developmental stage, in combination and/or sequentially [32]. During lactation, these cells expressed *ERα* and *PRLR* but *the epidermal growth factor receptor*, *IGF1R*, *TGFbR* at dry-off. Receptivity to PRL and estradiol during lactation is in accordance with the literature since PRL is known to be both a lactogenic and galactopoietic hormone [33, 34] and a recent study showed that estradiol would enhance the basal PRL exposure and *STAT5* expression [35]. At dry-off, the increase receptivity of luminal cells to *EGF, IGF1* and *TGFb* would be an indicator of an involute state of the mammary gland, an evolution of the tissue which involves an epithelial-to-mesenchymal transition, as was described in the mouse model [36].

At the beginning of our study, we have assumed that puberty is a key period during which the different lineages, basal/myoepithelial and luminal cells but also the progenitors and MaSC were committed to the branching morphogenesis process, making them highly identifiable. In line with this, the $CD49_f^{low}CD24^{pos}$ cell subpopulation was only found relatively abundant in the pubertal cows (18.6%). These cells were characterized by the expression of the basal protein CD10 and luminal markers *KRT7* and *CDH1*, an indicative characteristic of their belonging to both basal and luminal lineage. In addition, they overexpressed the *PR* and the proliferation marker *KI67*. From these data, one can hypothesize that the $CD49_f^{low}CD24^{pos}$ cells would be progenitors engaged in proliferation and exhibiting double lineage feature. This subpopulation, abundant at puberty and poorly present at lactation, slightly increased at dry-off as compared to lactation. Such a decrease of lineage-restricted progenitors then re-appearance of MaSC/progenitors with aging has already been reported in the mammary gland [37, 38].

Using standard methods for MaSC identification in several species including bovine [12, 17], we defined the $CD49_f^{high}CD24^{pos}$ as the putative bovine MaSC population. Here, the putative MaSC represented 3.3% of the total mammary cells at puberty, a small proportion in agreement with previous studies in mice and bovine [11, 13]. Interestingly, these cells consistently decreased from puberty (3.3% ±0.3) to lactation (1.5% ±0.5) and dry-off (0.4% ± 0.0). The molecular characteristics of the putative MaSC, however, remained very similar from one stage to another. They expressed the basal protein CD10 in accordance with a mouse study highlighting the basal feature of cells exhibiting stem cells functionalities [39]. Several genes were over-expressed by this cell subpopulation at all stages, including *$CD49_f$*, *CDH1* and the luminal keratins *KRT7* and *KRT8*. Therefore, in the present study, the putative MaSCs population displayed

luminal markers in addition to its basal phenotype. Consequently, this subpopulation appeared close to the luminal CD49$_f^{low}$CD24^{neg} cells in the PCA analysis, sharing some luminal characteristics. A luminal commitment of the putative MaSC could occurred postnatally, as it was described in mice [15, 16]. The notion that luminal cells that are hormone responsive expand and are maintained from luminal-restricted MaSC during the puberty and adult life led to presume a pool of MaSC dedicated to the luminal lineage. Consistent with this, we have showed that, at puberty, a sub-fraction of the CD49$_f^{high}$CD24^{pos} cells expressed KRT7 (suggesting a luminal commitment) in addition to the ubiquitous expression of KRT14 [14]. Interestingly, these cells also under-expressed several genes including *KI67* indicative of a low proliferative state. This, associated to an apparent low transcriptional activity (few genes expression) would represent a hallmark of quiescence which is a characteristic of stem cells.

As recently mentioned in the literature, it is difficult to find out a specific marker of the MaSC. Here, we looked at several stem cell markers including *LGR5*, *PROCR* and *NOTCH1*, and none were found overexpressed in the MaSC subpopulation, whatever the physiological stage. These MaSC markers, however, were characterize in rodents and may be species-specific. An alternative is that these markers are expressed at an early developmental stage such as embryogenesis but not postnatally in the adult MaSC.

To conclude, we showed that the luminal and basal/myoepithelial subpopulations (respectively the CD49$_f^{low}$CD24^{neg} and CD49$_f^{high}$CD24^{neg}) present characteristics in line with their function and activity in the mammary gland, the receptivity of the luminal cells differing totally at each stage. Unlike the luminal cells which did not vary in proportion, the basal cells clearly decreased at lactation and dry-off. Some of the epithelial cells were present during puberty and were absent during the other stages. This is the case for the CD49$_f^{low}$CD24^{pos} subpopulation hypothesized in our study to be progenitors and exhibiting proliferative as well as double lineage (luminal/basal) features. In contrast, the luminal CD49$_f^{med}$CD24^{neg} were only present during lactation, and accordingly, were characterized by expression of the milk constituents, including the caseins and α-lactalbumin indicating their secretory activity. On the other hand, the molecular characteristics of the putative MaSC defined as the CD49$_f^{high}$CD24^{pos} subpopulation did not evolve between physiological stages but their relative proportion did, being less abundant at dry-off and lactation than at puberty. On the basis of these results, we can assume that while animals become older their pool of MaSC decrease. We cannot exclude, however, that this pool of MaSC stay constant, the expression pattern of CD49$_f$ and CD24 by MaSC changing over time. Of note, after involution of the mammary gland and long period of dry-off we observed a slight increase of putative progenitors as well as of mature epithelial cells exhibiting high receptivity to remodeling factors. This study provides new insights on the bovine mammary epithelial cell lineage changes, both in terms of the relative proportion of the cell populations and their molecular features, through key periods of the animal life.

Material and Methods

Animals

All the animal procedures were discussed and approved by the CNREEA No. 07 (Local Ethics Committee in Animal Experiment of Rennes) in compliance with French regulations (Decree No. 2013–118, February 07, 2013). The Holstein cows (*Bos Taurus*) used in this study were housed at the INRA experimental farm of Mejusseaume (UMR PEGASE, Le Rheu, France) and sacrificed at the slaughterhouse of Gallais Viande (Montauban-de-Bretagne, France) following standard commercial practices. Three pubertal cows at 17 months of age, four multiparous lactating Holstein cows (4th and 6th lactation) producing 35 kg of milk/d and three dried Holstein cows at 6 years of dry-off were used in this study. Pubertal animals were those previously used to highlight the mammary epithelial populations at puberty [14]. The mammary glands were collected at the time of slaughter and immediately transported on ice to the laboratory to be sampled.

Mammary Tissue Sampling

Total mammary gland of pubertal cows was dissected and the whole parenchymal tissue above the teat was sampled. For lactating and dried cows, the parenchymal tissue was sampled in the middle udder at several areas of the secretory region. Samples destined for tissue dissociation were manually cut into small explants (≈1 mm^3), suspended in 90% fetal bovine serum (10270–106; Gibco Invitrogen Saint Aubin, France)/ 10% dimethyl sulfoxide (DMSO, D2650, Sigma-Aldrich, Saint-Quentin Fallavier, France) and stored at −150 °C. For immunohistological analysis, tissue pieces (≈ 5 mm3) were processed and embedded in paraffin as previously detailed [13].

Flow Cytometry and Cell Sorting

Mammary tissue fragments were thawed and enzymatically dissociated as previously described [13] to obtain a single cell suspension. Dissociated cells were incubated in MACS buffer with the relevant antibodies for 20 min at 4 °C in the dark, washed and re-suspended in MACS buffer (130-091-222, Miltenyi Biotec, Paris, France) with 2% bovine serum albumin (130-091-376; Miltenyi Biotec) for flow cytometry analysis or cell sorting. Flow cytometry was performed using a

MACSQuant Analyzer 10 cytometer (Miltenyi Biotec). The controls and gating strategy used in the present study have been previously detailed [13]. Note that isotype control antibodies were used as negative controls in the flow cytometry experiment. Data were analyzed using MACSQuantify analysis software (Miltenyi Biotec). For cell sorting, cells were incubated with the relevant antibodies. Single live cells were gated by DAPI exclusion and sorted on a BD FACS ARIA II flow cytometer (BIOSIT CytomeTRI technical Platform – Villejean Campus, Rennes, France). Sorted cells were pelleted at 300G for 5 min at 4 °C and stored at −80 °C. The antibodies used are described in supplemental Table S2.

mRNA Extraction and Quantitative PCR

RNA extraction was performed on sorted cells using the Nucleospin RNA XS kit (740,902, Macherey-Nagel, Hoerdt, France) according to the manufacter's instructions. RNA concentration and purity, evaluated from the A260/280 nm and A260/230 nm absorbance ratios, were measured on a NanoDrop ND-1000 spectrophotometer (NanoDrop Technologies, Wilmington, DE). Total RNA (500 ng) was subsequently reverse-transcribed using the VILO SuperScript kit (11754–050; Invitrogen, Paris, France) according to the manufacturer's recommendation. The resulting cDNA was used to test the expression of 48 genes with the Smartchip Real time PCR technology using the Wafergen Smartchip cycler and Smartchip Multisample Nanodipenser (Wafergen Biosystems; BIOSIT GEH Platform – Beaulieu Campus, Rennes, France). An efficiency and melt curves were integrated in the Smartchip run for each gene. The raw cycle threshold (Ct) values were transformed into quantities using the delta Ct method. This calculation of Delta Ct (Ct of target gene-Ct of reference genes mean) was chosen to highlight the level of expression for each cell subpopulation considered as independent subpopulations. The two most stable endogenous genes, the Ribosomal Protein Large P0 (*RPLP0)* and the Ribosomal Protein S5, were selected as control genes within a panel of three genes (*18S rRNA, Ribosomal Protein S5* and *RPLP0*) using the Normfinder algorithm. The mean of these endogenous control genes was used in the Delta Ct calculation to normalize the relative gene expression data. All primers used in this study are described in the supplemental Table S3.

Hematoxylin and eosin staining was performed on paraffin sections (8 μm) prepared from all animals used in this study ($n = 10$) as previously described [13]. Quantification of the areas occupied by the different tissue types, i.e. stroma, epithelium, fat and acini was determined from the scanned images generated by the NanoZoomer Digital Pathology technology (Hamamatsu, Kitse, Sweden) using macros in Image J software (1.48v version). Stromal tissue was referred to as the connective or fibrotic tissue (pink-colored area), including the vascular tissue, while the adipose tissue (white cells) was determined separately. The epithelium included the well-organized epithelial tissue areas (purple-colored). For each tissue type, data are expressed in percentage of the total area of the mammary section (area occupied by mammary tissue cells, i.e. without the area of the duct lumens). The sum of these tissue types (stromal, adipose and epithelial) accounted for 100%. The area occupied by acini was determined separately, including the area occupied by the acini lumen, and expressed as percent of the total area of the mammary section. Immunohistochemical staining was performed using paraffin sections (5 μm) as follows. After deparaffinization and rehydration, slides were incubated with 50 mM ammonium chloride (A0171, Sigma-Aldrich) for 10 min, with 0.1% Sudan black B (S2380, Sigma-Aldrich) in 70% ethanol for 20 min to quench the autofluorescence of immune cells and rinsed with Tris-buffered saline (TBS) 0.02% Tween-20 (P1379, Sigma-Aldrich). Tissue sections were subjected to heat-induced epitope retrieval twice in 1 mM ethylenediaminetetraacetic acid (EDTA, E9884, Sigma-Aldrich), pH 8 using a microwave at 800 watts for 5 min. Sections were permeabilized with 0.25% Triton X-100 (T9284, Sigma-Aldrich) and nonspecific-antibody binding was blocked with 2% bovine serum albumin (A2153, Sigma-Aldrich) in TBS. Tissue slices were then sequentially incubated with primary and secondary antibodies (Table S1) at 37 °C for 1 h30 and 45 min, respectively. After washing, nuclei were counterstained with Hoechst 33342 (14,533, VWR) at 1 μg/mL for 2 min. Slides were mounted using Vectashield mounting medium (H-1000; Vector Laboratories, Burlingame, CA). Images were acquired using an Apotome™ and the Zen software (Zeiss france).

Statistical Analysis

Data of flow cytometry and qPCR were expressed as means ± SEM. Data were subjected to analysis of variance (ANOVA) using the R Studio software. For statistical analysis of histological results, we used the non-parametric Mann-Whitney *U* test. Significant differences were considered at $p < 0.05$ and different letters indicate significant differences ($p < 0.05$). Data from qPCR were submitted to a multivariate analysis using a principal component analysis (PCA) with FactoMineR in R for the clustering of gene expression data pertaining for the differences observed in each subpopulation.

Acknowledgements This work was supported by the Animal Physiology & Livestock System Department of the French National Institute for Agricultural Research (INRA). We thank Laurent Deleurme and Gersende Lacombe from the CytomeTRI platform as well as Marine Biget from the GEH platform of the BIOSIT core facility at Rennes (France) for technical assistance. Acknowledgements are also extended to the staff at the INRA dairy farm of Méjusseaume (UMR1348 PEGASE, Le Rheu, France); Sandra Wiart and Frédérique Mayeur-Nickel for laboratory analyses and Rémi Resmond for technical assistance in statistics.

Author Contributions L. Finot and F. Dessauge designed and conceived experiments, L. Finot performed experiments, assemblied and analysed data. L. Finot, E.Chanat and F. Dessauge collaborated to the data interpretation. The three authors collaborated equally on the writing of the manuscript and its final approval.

Compliance with Ethical Standards

Conflict of Interest We declare no conflict of interest, no competing financial and non-financial interests

Publisher's Note Springer Nature remains neutral with regard to jurisdictional claims in published maps and institutional affiliations.

References

1. Akers RM, McFadden TB, Purup S, Vestergaard M, Sejrsen K, Capuco AV. Local IGF-I axis in peripubertal ruminant mammary development. J Mammary Gland Biol Neoplasia. [Research Support, Non-U.S. Gov't Research Support, U.S. Gov't, Non-P.H.S. Review]. 2000 Jan;5(1):43–51.
2. Woodward TL, Beal WE, Akers RM. Cell interactions in initiation of mammary epithelial proliferation by oestradiol and progesterone in prepubertal heifers. J Endocrinol. 1993 Jan;136(1):149–57.
3. Scheele CL, Hannezo E, Muraro MJ, Zomer A, Langedijk NS, van Oudenaarden A, et al. Identity and dynamics of mammary stem cells during branching morphogenesis. Nature. [Research Support, Non-U.S. Gov't]. 2017 Feb 16;542(7641):313–7.
4. Lee HJ, Ormandy CJ. Interplay between progesterone and prolactin in mammary development and implications for breast cancer. Molecular and cellular endocrinology. [Review]. 2012 Jun 24;357(1–2):101–7.
5. Watson CJ, Kreuzaler PA. Remodeling mechanisms of the mammary gland during involution. Int J Dev Biol. [Research Support, Non-U.S. Gov't Review]. 2011;55(7–9):757–62.
6. Capuco AV, Wood DL, Baldwin R, McLeod K, Paape MJ. Mammary cell number, proliferation, and apoptosis during a bovine lactation: relation to milk production and effect of bST. J Dairy Sci. 2001 Oct;84(10):2177–87.
7. Deome KB, Faulkin LJ Jr, Bern HA, Blair PB. Development of mammary tumors from hyperplastic alveolar nodules transplanted into gland-free mammary fat pads of female C3H mice. Cancer Res. 1959 Jun;19(5):515–20.
8. Ellis S, Capuco AV. Cell proliferation in bovine mammary epithelium: identification of the primary proliferative cell population. Tissue Cell. [Research Support, U.S. Gov't, Non-P.H.S.]. 2002 Jun;34(3):155–63.
9. Capuco AV. Identification of putative bovine mammary epithelial stem cells by their retention of labeled DNA strands. Exp Biol Med (Maywood). [Research Support, U.S. Gov't, Non-P.H.S.]. 2007 Nov;232(10):1381–90.
10. Martignani E, Eirew P, Eaves C, Baratta M. Functional identification of bovine mammary epithelial stem/progenitor cells. Vet Res Commun. [Research Support, Non-U.S. Gov't]. 2009 Sep;33 Suppl 1:101–3.
11. Osinska E, Wicik Z, Godlewski MM, Pawlowski K, Majewska A, Mucha J, et al. Comparison of stem/progenitor cell number and transcriptomic profile in the mammary tissue of dairy and beef breed heifers. J Appl Genet. [Research Support, Non-U.S. Gov't]. 2014 Aug;55(3):383–95.
12. Rauner G, Barash I. Cell hierarchy and lineage commitment in the bovine mammary gland. PLoS One. [Research Support, Non-U.S. Gov't]. 2012;7(1):e30113.
13. Perruchot MH, Arevalo-Turrubiarte M, Dufreneix F, Finot L, Lollivier V, Chanat E, et al. Mammary epithelial cell hierarchy in the dairy cow throughout lactation. Stem Cells Dev. 2016 Oct 01;25(19):1407–18.
14. Finot L, Chanat E, Dessauge F. Molecular signature of the putative stem/progenitor cells committed to the development of the bovine mammary gland at puberty. Sci Rep. 2018 Nov 1;8(1):16194.
15. Van Keymeulen A, Rocha AS, Ousset M, Beck B, Bouvencourt G, Rock J, et al. Distinct stem cells contribute to mammary gland development and maintenance. Nature. [Research Support, Non-U.S. Gov't]. 2011 Oct 09;479(7372):189–93.
16. Rodilla V, Dasti A, Huyghe M, Lafkas D, Laurent C, Reyal F, et al. Luminal progenitors restrict their lineage potential during mammary gland development. PLoS Biol. [Research Support, Non-U.S. Gov't]. 2015 Feb;13(2):e1002069.
17. Rauner G, Ledet MM, Van de Walle GR. Conserved and variable: Understanding mammary stem cells across species. Cytometry A. [Review]. 2017 Aug 22.
18. Fu N, Lindeman GJ, Visvader JE. The mammary stem cell hierarchy. Curr Top Dev Biol. [Research Support, Non-U.S. Gov't Review]. 2014;107:133–60.
19. Sleeman KE, Kendrick H, Ashworth A, Isacke CM, Smalley MJ. CD24 staining of mouse mammary gland cells defines luminal epithelial, myoepithelial/basal and non-epithelial cells. Breast Cancer Res. [Research Support, Non-U.S. Gov't]. 2006;8(1):R7.
20. Oakes SR, Gallego-Ortega D, Ormandy CJ. The mammary cellular hierarchy and breast cancer. Cell Mol Life Sci. [Review]. 2014 Nov;71(22):4301–24.
21. Shackleton M, Vaillant F, Simpson KJ, Stingl J, Smyth GK, Asselin-Labat ML, et al. Generation of a functional mammary gland from a single stem cell. Nature. [Research Support, Non-U.S. Gov't]. 2006 Jan 05;439(7072):84–8.
22. Stingl J, Eirew P, Ricketson I, Shackleton M, Vaillant F, Choi D, et al. Purification and unique properties of mammary epithelial stem cells. Nature. [Research Support, Non-U.S. Gov't]. 2006 Feb 23;439(7079):993–7.
23. Finot L, Chanat E, Dessauge F. Molecular signature of the putative stem/progenitor cells committed to the development of the bovine mammary gland at puberty. Sci Rep. 2018;submitted.
24. Safayi S, Korn N, Bertram A, Akers RM, Capuco AV, Pratt SL, et al. Myoepithelial cell differentiation markers in prepubertal bovine mammary gland: effect of ovariectomy. J Dairy Sci. [Research Support, U.S. Gov't, Non-P.H.S.]. 2012 Jun;95(6):2965–76.
25. Stingl J, Raouf A, Emerman JT, Eaves CJ. Epithelial progenitors in the normal human mammary gland. Journal of mammary gland biology and neoplasia. [Research Support, Non-U.S. Gov't Review]. 2005 Jan;10(1):49–59.
26. Trejo CL, Luna G, Dravis C, Spike BT, Wahl GM. Lgr5 is a marker for fetal mammary stem cells, but is not essential for stem cell activity or tumorigenesis. NPJ Breast Cancer. 2017;3:16.
27. Wang D, Cai C, Dong X, Yu QC, Zhang XO, Yang L, et al. Identification of multipotent mammary stem cells by protein C receptor expression. Nature. [Research Support, Non-U.S. Gov't]. 2015 Jan 01;517(7532):81–4.
28. Ewald AJ, Brenot A, Duong M, Chan BS, Werb Z. Collective epithelial migration and cell rearrangements drive mammary branching morphogenesis. Dev Cell. [Research Support, N.I.H., Extramural Research Support, Non-U.S. Gov't]. 2008 Apr;14(4):570–81.
29. Deugnier MA, Moiseyeva EP, Thiery JP, Glukhova M. Myoepithelial cell differentiation in the developing mammary gland: progressive acquisition of smooth muscle phenotype. Dev Dyn. [Research Support, Non-U.S. Gov't]. 1995 Oct;204(2):107–17.

30. Capuco AV, Akers RM. Mammary involution in dairy animals. J Mammary Gland Biol Neoplasia. [Review]. 1999 Apr;4(2):137–44.
31. Pelissier FA, Garbe JC, Ananthanarayanan B, Miyano M, Lin C, Jokela T, et al. Age-related dysfunction in mechanotransduction impairs differentiation of human mammary epithelial progenitors. Cell Rep. [Research Support, N.I.H., Extramural Research Support, Non-U.S. Gov't Research Support, U.S. Gov't, Non-P.H.S.]. 2014 Jun 26;7(6):1926–39.
32. Berryhill GE, Trott JF, Hovey RC. Mammary gland development–It's not just about estrogen. J Dairy Sci. [Research Support, N.I.H., Extramural Research Support, U.S. Gov't, Non-P.H.S. Review]. 2016 Jan;99(1):875–83.
33. Akers RM. A 100-year review: mammary development and lactation. J Dairy Sci. 2017 Dec;100(12):10332–52.
34. Lollivier V, Lacasse P, Angulo Arizala J, Lamberton P, Wiart S, Portanguen J, et al. In vivo inhibition followed by exogenous supplementation demonstrates galactopoietic effects of prolactin on mammary tissue and milk production in dairy cows. J Dairy Sci. 2015 Dec;98(12):8775–87.
35. Tong JJ, Thompson IM, Zhao X, Lacasse P. Effect of 17beta-estradiol on milk production, hormone secretion, and mammary gland gene expression in dairy cows. J Dairy Sci. 2018 Mar;101(3):2588–601.
36. Faure E, Heisterkamp N, Groffen J, Kaartinen V. Differential expression of TGF-beta isoforms during postlactational mammary gland involution. Cell Tissue Res. [Research Support, Non-U.S. Gov't Research Support, U.S. Gov't, P.H.S.]. 2000 Apr;300(1):89–95.
37. Wu A, Dong Q, Gao H, Shi Y, Chen Y, Zhang F, et al. Characterization of mammary epithelial stem/progenitor cells and their changes with aging in common marmosets. Sci Rep. 2016 Aug 25;6:32190.
38. Garbe JC, Pepin F, Pelissier FA, Sputova K, Fridriksdottir AJ, Guo DE, et al. Accumulation of multipotent progenitors with a basal differentiation bias during aging of human mammary epithelia. Cancer Res. [Research Support, N.I.H., Extramural Research Support, U.S. Gov't, Non-P.H.S.]. 2012 Jul 15;72(14):3687–701.
39. Prater MD, Petit V, Alasdair Russell I, Giraddi RR, Shehata M, Menon S, et al. Mammary stem cells have myoepithelial cell properties. Nat Cell Biol. 2014 Oct;16(10):942–50 1-7.